Send Orders for Reprints to reprints@benthamscience.net

Current Inorganic Chemistry, 2013, *3*, 161-171

Slow Magnetization Relaxation in a 1-D Double-Chain Coordination Polymer Composed of $\{Dy^{III}_4\}$ Repeating Units

Dimitris I. Alexandropoulos[1], Chaoran Li[2], Catherine P. Raptopoulou[3], Vassilis Psycharis[3], Wolfgang Wernsdorfer[4], George Christou[2] and Theocharis C. Stamatatos[1,*]

[1]*Department of Chemistry, Brock University, L2S 3A1 St. Catharines, Ontario, Canada*

[2]*Department of Chemistry, University of Florida, Gainesville, Florida 32611-7200, USA*

[3]*Institute of Advanced Materials, Physicochemical Processes, Nanotechnology and Microsystems, Department of Materials Science, NCSR "Demokritos", 153 10 Aghia Paraskevi Attikis, Greece*

[4]*Institut Néel, CNRS, Nanoscience Department, BP 166, 380412 Grenoble Cedex 9, France*

Abstract: The "unsuccessful" synthesis of the non-commercially available '$Dy(O_2CPh)_3$' precursor from the stoichiometric reaction of $Dy(NO_3)_3{\cdot}5H_2O$ with 3 equivalents of NaO_2CPh in $MeCN/H_2O$ has led instead to the "successful" isolation and structural characterization of the 1-D coordination polymer $[Dy_4(O_2CPh)_{12}(H_2O)_8]_n{\cdot}2n(PhCO_2H){\cdot}n(MeCN)$ (**1**$\cdot 2n(PhCO_2H){\cdot}n(MeCN)$) in excellent yields (~90%). The one-dimensional double-chain structure of **1** was resulted from the linkage of two parallel chains by *syn,anti*-$\eta^1{:}\eta^1{:}\mu$ $PhCO_2^-$ groups. The lattice structure of **1** is further extended to a 2-D network through hydrogen bonding and π-π stacking interactions. The observation of out-of-phase (χ''_M) ac susceptibility signals suggested that **1** might be a molecular nanomagnet, and this was confirmed by single-crystal magnetization *vs.* dc field sweeps that exhibited hysteresis, the diagnostic property of a magnet.

Keywords: Carboxylates, coordination polymers, crystal structures, dysprosium, slow magnetization relaxation.

1. INTRODUCTION

Lanthanide (Ln) coordination chemistry has been attracting the interest of many research groups during the last two decades [1]. This is mainly due to the fact that both 0-D polynuclear complexes (molecular clusters) and multidimensional (1-, 2-, or 3-D) coordination polymers of 4f-metal ions possess beautiful structural motifs and intriguing physical (magnetic, catalytic and optical) properties [2]. Particularly in coordination polymers and molecular clusters, it is the nature and kind of the bridging organic ligand(s) which allow for the large diversity in the topologies and possible properties of the metal-organic coordination networks. By carefully selecting the ligand and the metal ion, scientists aim to tune the physical properties and thus realize various applications of coordination polymers in molecular magnetism, catalysis, electrical conductivity, luminescence, nonlinear optics, molecular electronics, drug delivery, and sensing [3]. The ultimate goal is the transformation of some coordination polymers and clusters to functional materials [4].

Towards this end, of particular interest is the ability of 4f-metal complexes (monomers, clusters, and coordination polymers) to act either as single-molecule magnets (SMMs) in a molecular level [5] or as single-chain magnets (SCMs) when the molecular species are covalently linked into 1-D chains [6]. In the former field, SMMs derive their properties from the combination of a large magnetic moment in the ground state with a large Ising-type magnetoanisotropy (negative zero-field splitting parameter, D). As a result, 4f-SMMs often possess a significant barrier to magnetization relaxation and at low enough temperatures they display out-of-phase ac magnetic susceptibility (χ_M'') signals, and hysteresis in magnetization vs. applied dc field loops. In case of SCMs, such species possess a large uniaxial anisotropy, strong intra-chain exchange interactions without spin compensation between the high-spin magnetic units, and good isolation of the chains in order to avoid two- and three-dimensional ordering; these lead to an upper limit to the relaxation barrier (Δ) given by $(D+4J)S^2$, where J is the interaction between repeating units of the chain. Thus, both SMMs and SCMs have been proposed for several potential applications, such as in very high-density information storage at the molecular level [7] and as qubits in quantum computation and spintronics [8].

The chances of identifying novel types of 4f-metal clusters or coordination polymers with enhanced or new magnetic properties will benefit from the development of new reaction systems with suitable organic ligands or combinations of organic and inorganic ligands [9]. Therefore, simple monocarboxylate groups (RCO_2^-; R = various) appear to be invaluable such ligands [10] due to their (i) affinity in binding to the oxophilic Ln^{III} ions by containing O-donor atoms, (ii) ability to bridge many metal centers under a variety of different modes (i.e., *syn,syn*, *syn,anti*, *anti,anti*), and (iii) position as magnetic couplers in promoting magnetic exchange interactions between the metal atoms they bridge

*Address correspondence to this author at the Department of Chemistry, Brock University, L2S 3A1 St. Catharines, Ontario, Canada;
Tel: +1-905-6885550; E-mail: tstamatatos@brocku.ca

1877-945X/13 $58.00+.00

[11]. The choice of the 4f-metal ion is also of great importance because it directs the interest regarding the potential applications. Thus, the significant spin and large anisotropy of the Dy^{III} ion renders it as an excellent candidate for the construction of novel lanthanide-based molecular magnetic materials [2, 9].

In an attempt to synthesize simple, non-commercially available, 4f-metal carboxylate precursors, which are excellent starting materials for the further synthesis of polynuclear metal complexes and coordination polymers [10, 12], we came across the unexpected formation (in almost quantitative yields) of a new one-dimensional coordination polymer with a double-chain architecture consisting of $\{Dy^{III}_4\}$ repeating units. The synthesis, structure, and magnetic properties of the isolated $[Dy_4(O_2CPh)_{12}(H_2O)_8]_n$ polymer are described in the present work; this compound can be considered as a useful starting material for further Ln^{III} carboxylate chemistry.

2. EXPERIMENTAL

2.1. General and Physical Measurements

Infrared (IR) spectrum was recorded in the solid state (KBr pellet) on a Perkin-Elmer 16 PC FT spectrometer in the 4000-450 cm^{-1} range. Elemental analyses (C, H, and N) were performed on a Perkin-Elmer 2400 Series II Analyzer. Direct current (dc) and alternating current (ac) magnetic susceptibility studies were performed at the University of Florida, Chemistry Department on a Quantum Design MPMS-XL SQUID susceptometer equipped with a 7 T magnet and operating in the 1.8-400 K range. Samples were embedded in solid eicosane to prevent torquing. Ac magnetic susceptibility measurements were performed in an oscillating ac field of 3.5 G and a zero dc field. The oscillation frequencies were in the 50-1000 Hz range. Pascal's constants were used to estimate the diamagnetic correction, which was subtracted from the experimental susceptibility to give the molar paramagnetic susceptibility (χ_M). Low-temperature (< 1.8 K) hysteresis loops were performed at Grenoble using an array of micro-SQUIDS [13]. The high sensitivity of this magnetometer allows the study of single crystals of SMMs and SCMs of the order of 10-500 μm. The field can be applied in any direction by separately driving three orthogonal coils.

2.2. Synthesis

2.2.1. $[Dy_4(O_2CPh)_{12}(H_2O)_8]_n \cdot 2n(PhCO_2H) \cdot n(MeCN)$ ($1 \cdot 2n(PhCO_2H) \cdot n(MeCN)$)

To a stirred, colorless solution of NaO_2CPh (0.43 g, 3.0 mmol) in $MeCN/H_2O$ (25 mL, 5:1 v/v) was added solid $Dy(NO_3)_3 \cdot 5H_2O$ (0.44 g, 1.0 mmol). The resulting solution was stirred for 1 h, during which time all the solids dissolved and the color of the solution changed to yellowish. The latter solution was filtered, and the filtrate was allowed to slowly evaporate at room temperature. After 6 days, X-ray quality colorless crystals of **1**·2*n*($PhCO_2H$)·*n*(MeCN) had appeared and were collected by filtration, washed with cold MeCN (2 x 3 mL), and dried under vacuum; the yield was 90%. Anal. Calcd for **1**·2$PhCO_2H$·2H_2O: C, 46.57; H, 3.67 %. Found: C, 46.18; H, 3.19 %. Selected IR data (cm^{-1}): 3390 (mb), 3058 (m), 1694 (m), 1598 (s), 1534 (vs), 1418 (vs), 1234 (m), 1172 (w), 1070 (w), 1024 (w), 938 (w), 854 (w), 816 (w), 718 (s), 552 (m), 428 (w).

Table 1. Crystallographic data for complex 1·2*n*($PhCO_2H$)·*n*(MeCN)

Parameter	1·2$PhCO_2H$·MeCN
Formula	$C_{100}H_{91}Dy_4NO_{36}$
M / g mol^{-1}	2532.74
Crystal system	triclinic
Space group	$P\bar{1}$
a / Å	10.0112(2)
b / Å	15.1833(2)
c / Å	16.7355(3)
α / °	110.278(1)
β / °	94.845(1)
γ / °	97.927(1)
V / $Å^3$	2339.31(7)
Z	1
T / K	160(2)
λ / Å	1.54178[a]
ρ_{calc} / g cm^{-3}	1.798
μ / mm^{-1}	17.568
Measd / independent (R_{int}) reflns	28566 / 7480 (0.0692)
Obsd reflns [$I > 2\sigma(I)$]	5198
R_1[b,c]	0.0448
wR_2[d]	0.0998
GOF on F^2	1.049
$(\Delta\rho)_{max,min}$ / e $Å^{-3}$	1.363, -1.588

[a] Cu-Kα radiation, graphite monochromator. [b] $I > 2\sigma(I)$. [c] $R_1 = \Sigma(||F_o| - |F_c||)/\Sigma|F_o|$. [d] $wR_2 = [\Sigma[w(F_o^2 - F_c^2)^2]/\Sigma[w(F_o^2)^2]]^{1/2}$, $w = 1/[\sigma^2(F_o^2) + [(ap)^2 + bp]$, where $p = [\max(F_o^2, 0) + 2F_c^2]/3$.

2.3. Single-crystal X-ray Crystallography

A colorless crystal of 1·2*n*($PhCO_2H$)·*n*(MeCN) (0.06 x 0.12 x 0.23 mm) was taken from the mother liquor and immediately cooled to -113 °C. Diffraction measurements were made on a Rigaku R-AXIS SPIDER Image Plate diffractometer using graphite monochromated Cu Kα radiation. Data collection (ω-scans) and processing (cell refinement, data reduction and Empirical absorption correction) were performed using the CrystalClear program package [14]. The structure was solved by direct methods using SHELXS-97 [15] and refined on F^2 by full-matrix least squares techniques with SHELXL-97 [16]. Hydrogen atoms were introduced at calculated positions as riding on bonded atoms. All non-H atoms were refined anisotropically. The programs used for molecular graphics were MERCURY [17] and DIAMOND [18]. Unit cell parameters and structure solution and refinement data for the complex are listed in Table **1**. Further crys-

Table 2. Selected Bond Lengths (Å) for the 1-D Coordination Polymer 1[a]

Dy1…Dy2	5.087(3)	Dy1-O6′	2.412(3)
Dy1…Dy2′	5.846(3)	Dy1-O9	2.287(4)
Dy1…Dy1′	7.103(3)	Dy1-O12#	2.314(4)
Dy2…Dy2′	8.347(6)	Dy2-O1##	2.275(4)
Dy1…Dy2#	4.925(3)	Dy2-O4W	2.401(3)
Dy1…Dy1″	8.129(5)	Dy2-O4	2.308(4)
Dy2′…Dy2#	7.127(3)	Dy2-O5	2.490(3)
Dy1-O1W	2.445(3)	Dy2-O7	2.480(3)
Dy1-O2W	2.478(3)	Dy2-O8	2.504(3)
Dy1-O2	2.312(4)	Dy2-O10	2.240(4)
Dy1-O3W	2.470(4)	Dy2-O11	2.295(4)
Dy1-O3	2.321(4)		

[a] The symbols of all symmetry operators are the same as in Figures 1 and 2.

tallographic details can be found in the CIF file provided in the Supporting Information.

3. RESULTS AND DISCUSSION

3.1. Synthetic Comments and IR Spectroscopy

Many synthetic procedures to polynuclear metal complexes and coordination polymers rely on the reactions of simple metal sources, such as metal halides, carboxylates or β-diketonates, with a potentially chelating/bridging organic ligand. This route was also known from our previous work [19], as well as the work from other research groups [9, 20], to yield structurally and magnetically interesting 4f-metal complexes using a variety of different alkoxide- or oximate-based ligands. Given the lack of many commercially available 4f-metal carboxylate sources, other than the $Ln(O_2CMe)_3$ ones, we have attempted in the present study to synthesize and isolate in high yields the analogous $Ln(O_2CPh)_3$ precursors in order to react them with various chelating/bridging ligands. We initiated our efforts by following the rational synthetic protocol [21] and thus reacting stoichiometric amounts of the commercially available $Dy(NO_3)_3{\cdot}5H_2O$ with 3 equivalents of NaO_2CPh in a solvent mixture comprising MeCN and H_2O. We anticipated the immediate precipitation of the desired '$Dy(O_2CPh)_3$', as has been the case in several transition metal benzoate salts, $M(O_2CPh)_2{\cdot}xH_2O$ (M^{II} = Mn, Co, Ni, Cu; x = 2-4). Instead, we came across the observation of a yellowish solution which retained its colour and form even after prolonged magnetic stirring times at room temperature. To our surprise, slow evaporation of the yellowish solution led to the subsequent isolation of well-formed colorless, plate-like crystals of the complex $[Dy_4(O_2CPh)_{12}(H_2O)_8]_n{\cdot}2n(PhCO_2H){\cdot}n$(Me-CN) (**1**·2*n*($PhCO_2H$)·*n*(MeCN)), which is a 1-D coordination polymer composed of {Dy_4} repeating units (*vide infra*), in excellent yield (~90%). The formation of **1** is summarized in Eq. (1).

$$4n\ Dy(NO_3)_3{\cdot}5H_2O + 12n\ NaO_2CPh \xrightarrow{MeCN\ /\ H_2O} [Dy_4(O_2CPh)_{12}(H_2O)_8]_n + 12n\ NaNO_3 + 12n\ H_2O \quad (1)$$

1

It is useful to mention that the addition of adequate amounts of H_2O (3-7 mL) in the reaction mixture is essential for the dissolution of both starting materials and to ensure the non-contamination of the crystalline solid **1** with the water-soluble $NaNO_3$ salt. IR spectroscopy on single-crystals of **1** confirmed the absence of any bands (i.e., 1380-1385 cm^{-1}) that would correspond to the presence of a D_{3h} ionic nitrate [22]. Finally, compound **1** is a stable, crystalline solid at room temperature, soluble in MeOH, DMF and DMSO, partially soluble in MeCN, H_2O and $MeNO_2$, and insoluble in all common non-polar organic solvents such as $CHCl_3$, benzene, and toluene.

The presence of both neutral benzoic acid in the crystal lattice and coordinated H_2O molecules in **1**·2*n*($PhCO_2H$)·*n*(MeCN) is manifested by a broad IR band of medium intensity at 3390 cm^{-1}, assigned to $\nu(OH)_{benzoic}/\nu(OH)_{water}$; the broadness and relatively low frequency of this band are both indicative of strong hydrogen bonding (*vide infra*) [23]. The ν(C=O) mode of the neutral benzoic acid lattice molecules is found at 1694 cm^{-1} in the spectrum of **1**·2*n*($PhCO_2H$)·*n*(MeCN), lower than the wavenumber expected for a free carbonyl group in $PhCO_2H$ (~1720-1750 cm^{-1}); this shift is consistent with the involvement of the ketone-O atom in hydrogen bonding interactions [24]. The very strong bands at 1534 and 1418 cm^{-1} in the spectrum of **1** can be assigned to the $\nu_{as}(CO_2)$ and $\nu_s(CO_2)$ modes, respectively, of the bound benzoate groups. The difference Δ [$\Delta = \nu_{as}(CO_2) - \nu_s(CO_2)$] is 116 cm^{-1}, much less than the corresponding value for NaO_2CPh (184 cm^{-1}), as expected from the predominant bidentate bridging mode of the carboxylate groups in **1** [23, 24].

3.2. Description of Structure

Complex **1**·2*n*($PhCO_2H$)·*n*(MeCN) crystallizes in the triclinic space group $P\bar{1}$. Its crystal structure is composed of $[Dy_4(O_2CPh)_{12}(H_2O)_8]$ repeating units (Fig. **1**, right) arranged in an overall 1-D double-chain, and lattice benzoic acid and MeCN molecules of crystallization; the latter two will be briefly discussed in the supramolecular description of **1**. Selected interatomic distances for **1** are listed in Table **2**.

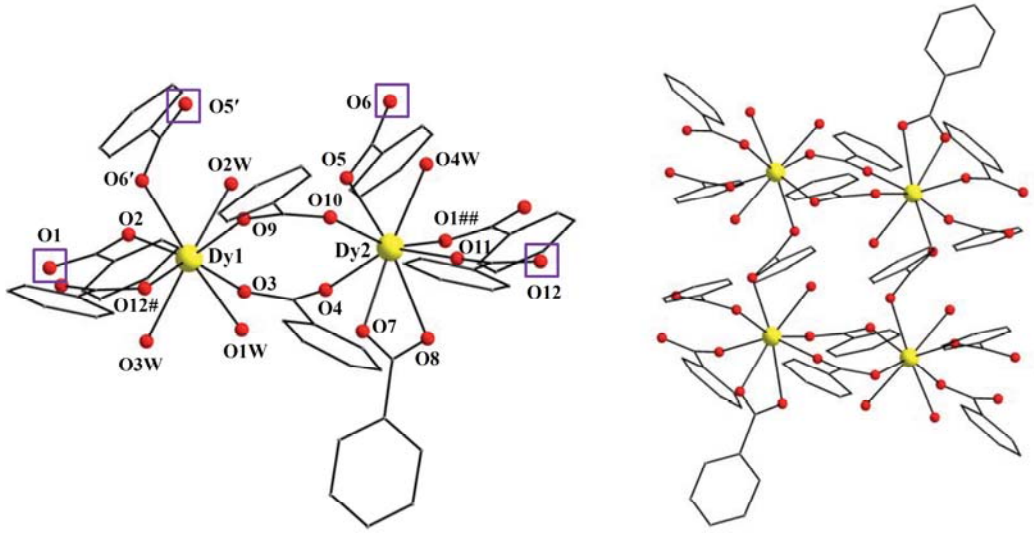

Fig. (1). (left) Partially labeled PovRay representation of the asymmetric unit of **1**. The atoms within the colored squares indicate the connection points at which the 1-D, single- (O1 and O12) and double- (O5′ and O6) chains are extended. Color code: Dy^{III} yellow, O red, C gray. Symmetry code: ′ = 1-*x*, 1-*y*, -*z*; # = -1+*x*, *y*, *z*; ## = 1+*x*, *y*, *z*. (right) The $\{Dy_4\}$ repeating unit of the double-chain **1**.

The asymmetric unit of **1** consists of two crystallographically unique Dy^{III} atoms (Dy1 and Dy2) which are bridged together by the oxygen atoms (O3, O4, O9 and O10) of two *syn,syn*-η^1:η^1:μ $PhCO_2^-$ groups (Fig. **1**, left). The Dy1···Dy2 distance within the asymmetric unit is 5.087(3) Å. The dinuclear asymmetric unit is further linked to adjacent dimers through the oxygen atoms of four *syn,syn*-η^1:η^1:μ $PhCO_2^-$ groups (defined by O1/O2 and O11/O12) resulting in the formation of a linear chain (named **A**) that runs parallel to the *a*-axis. The Dy1···Dy2 distance through this type of bridging is 4.925(3) Å. Both Dy atoms are eight-coordinate with their coordination spheres completed by three terminal water molecules (O1W, O2W and O3W) on Dy1, and a bidentate chelating $PhCO_2^-$ group (O7 and O8) and a terminal H_2O molecule (O4W) on Dy2. In addition, the oxygen atoms of two *syn,anti*-η^1:η^1:μ $PhCO_2^-$ groups (O5, O6, and their symmetry-related counterparts) serve to link the linear chain **A** with a second, symmetry-related and structurally-identical, one (named **B**), yielding an overall one-dimensional double-chain polymer of $[Dy_4(O_2CPh)_{12}(H_2O)_8]$ repeating units (Fig. **2**, top). The Dy1···Dy2 distance through this type of bridging is 5.846(3) Å. The two single-chains **A** and **B** are parallel to each other, whereas the tetranuclear $\{Dy_4\}$ units of the double-chain form rhombus-shaped domains (Fig. **2**, bottom).

To estimate the closer coordination polyhedra defined by the donor atoms around Dy1 and Dy2 in the asymmetric unit of **1**, a comparison of the experimental structural data with the theoretical data for the most common polyhedral structures with 8 vertices was performed by means of the program SHAPE [25]. Following the proposal by Avnir and co-workers [26] to consider symmetry and polyhedral shape as continuous properties that can be quantified from structural data, Alvarez and co-workers have applied these concepts and the associated methodology to the stereochemical analysis of very large sets of molecular structures, including systems with 8-vertex polyhedral [27]. The so-called Continuous Shape Measures (CShM) approach essentially allows one to numerically evaluate by how much a particular structure deviates from an ideal shape [28]. There are many polyhedra with eight vertices such as Platonic solids (cube), Archimedean or Catalan (triakis tetrahedron) solids and others such as triangular dodecahedra. In addition, prisms (biaugmented trigonal) or antiprisms (square antiprism) can be made with eight vertices as well as many semiregular three-dimensional figures. The most common of these [27], which will be considered here, are the octagon, the heptagonal pyramid, the hexagonal bipyramid and the four Johnson polyhedra (gyrobifastigium, elongated triangular bipyramid, biaugmented trigonal prism and snub tetrahedron). The best fit (Table **3**) was obtained for the square antiprism (Dy1; Fig. **3**, left) and triangular dodecahedron (Dy2; Fig. (**3**), right), with the two faces consisting of atoms O2, O3W, O6, O12 and O9, O1W, O3, O2W (for Dy1) and O1, O7, O8, O11 and O4, O4W, O5, O10 (for Dy2).

The lattice structure of **1** is built through hydrogen bonding and π-π stacking interactions. The lattice benzoic acid molecules (defined by C44-C49 atoms) are hanged on both sides of the double-chains of **1** through the hydrogen bonds developed between O13 and O14 carboxylate oxygen atoms and O7 and O1W atoms belonging to the chain part of the structure (O14···O7 and O13···O1W hydrogen bonds, Fig. (**4**) (top), Table **4**). MeCN solvate molecules are also hydrogen bonded to the double chain through O3W···N1 hydrogen bonds (Fig. **4** (top), Table **4**). All the remaining hydrogen bonding interactions, listed in Table **4** and shown in Fig. (**4**), are generated within the double-chains of **1**. The lattice benzoic acid molecules serve as bridges for neighboring double chains extended parallel to the *a* crystallographic axis. The carboxylate side of these molecules develops the hydrogen bonds described above with one chain and the other side of the molecule defined by the phenyl ring (atoms C44-C49) develops weak π-π interactions with aromatic rings of the bonded $PhCO_2^-$ groups to a neighboring double chain defined by C37-C42 phenyl ring atoms. The angle between the two mean planes is 15.7° and the distance between the two centroids is 4.081 Å (Fig. **4**, bottom). Through these links of neighboring double-chains, an overall 2-D network is built parallel to the (0 1 -1) crystallographic planes.

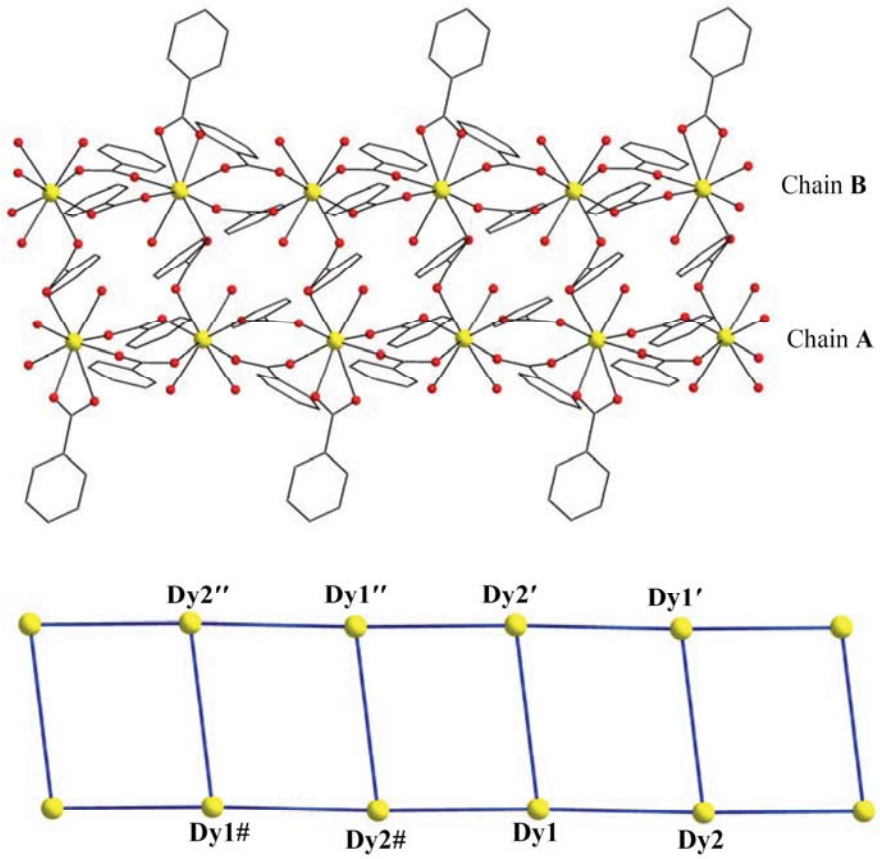

Fig. (2). (top) A portion of the 1-D double-chain of **1** formed parallel to the *a* axis. The lattice molecules have been omitted for clarity. (bottom) The rhombus-shaped domains within **1**; the blue thick lines indicate the Dy…Dy vectors. Color code: Dy^{III} yellow, O red, C gray. Symmetry code: ′ = 1-*x*, 1-*y*, -*z*; ″ = -*x*, 1-*y*, -*z*; # = -1+*x*, *y*, *z*.

Table 3. Shape Measures of the 8-coordinate Dy1[a] and Dy2[a] Coordination Polyhedra in 1. The Values in Boldface Indicate the Closest Polyhedron According to the Continuous Shape Measures

Polyhedron[b]	Dy1	Dy2
OP-8	28.73	30.79
HPY-8	23.61	22.15
HBPY-8	15.74	13.09
CU-8	8.69	13.92
SAPR-8	**0.87**	4.22
TDD-8	0.92	**1.63**
JGBF-8	14.88	9.51
JETBPY-8	26.79	27.65
JBTPR-8	2.03	3.20
BTPR-8	1.78	3.10
JSD-8	2.83	2.02
TT-8	9.13	14.53
ETBPY-8	22.45	23.93

[a]See Figure 3; [b] Abbreviations: OP-8, octagon; HPY-8, heptagonal pyramid; HBPY-8, hexagonal bipyramid; CU-8, cube; SAPR-8, square antiprism; TDD-8, triangular dodecahedron; JGBF-8, Johnson gyrobifastigium; JETBPY-8, Johnson elongated triangular bipyramid; JBTPR-8, Johnson biaugmented trigonal prism; BTPR-8, biaugmented trigonal prism; JSD-8, Johnson snub diphenoid; TT-8, triakis tetrahedron; ETBPY-8, elongated trigonal bipyramid.

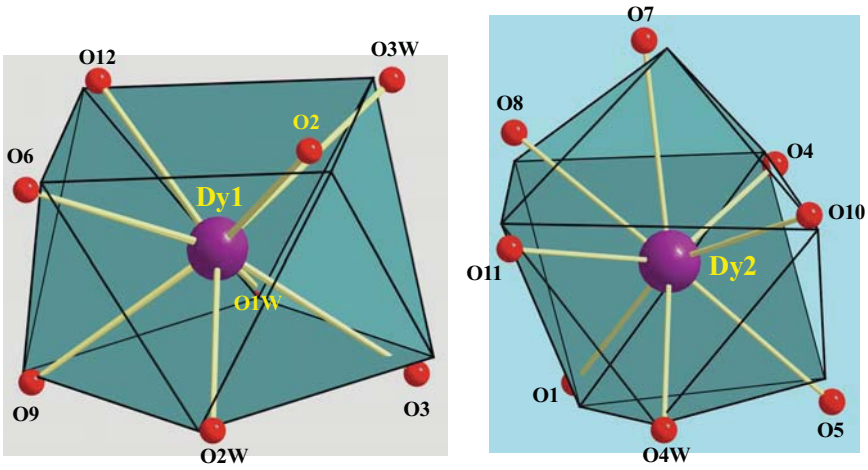

Fig. (3). Square antiprismatic coordination sphere of Dy1 (left) and triangular dodecahedral geometry of Dy2 (right) in the structure of **1**. The points connected by the black lines define the vertices of the ideal polyhedron.

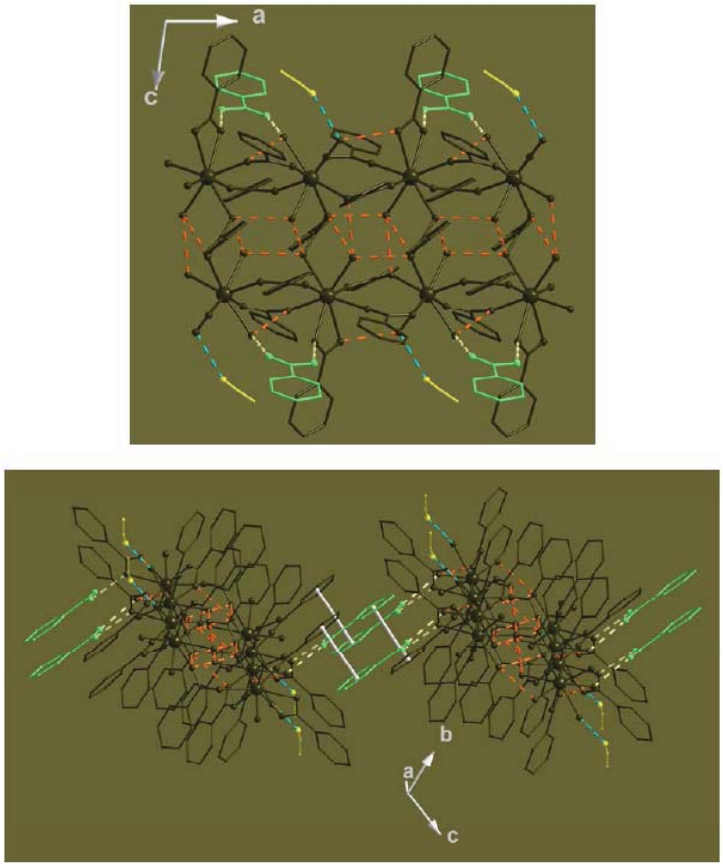

Fig. (4). (top) A small part of a double-chain of **1** with lattice $PhCO_2H$ (light green) and MeCN (yellow) molecules hanged through O···O and O···N hydrogen bonding interactions (dashed light green and blue lines, respectively). (bottom) A small portion of the 2-D network of **1** formed by π-π stacking interactions (white lines) which are shown as parallel to *a*-axis. In both figures, the intra-chain hydrogen bonding interactions are shown as dashed orange lines.

Table 4. Hydrogen Bonds in 1·2*n*($PhCO_2H$)·*n*(MeCN)

Interaction	D···A (Å)	H···A (Å)	D-H···A (°)	Symmetry Operation
O(14)-H(14O)···O(7)	2.674	1.878	157.8	x, y, z
O(1W)-H(1WA)···O(13)	2.801	1.983	144.6	x, y, z

Table 4. contd…

Interaction	D···A (Å)	H···A (Å)	D-H···A (°)	Symmetry Operation
O(3W)-H(3WA)···N(1)	2.847	2.286	123.4	x, y, z
O(1W)-H(1WB)···O(4)	2.955	2.272	137.2	x, y, z
O(2W)-H(2WA)···O(5)	2.924	2.093	170.0	x, y, z
O(2W)-H(2WB)···O(5)	2.912	2.140	144.8	x, y, z
O(3W)-H(3WB)···O(8)	2.947	2.128	163.7	-1+x, y, z
O(4W)-H(4WA)···O(2)	3.015	2.231	154.8	1-x, 1-y, -z
O(4W)-H(4WA)···O(6)	2.882	2.270	129.6	x, y, z
O(4W)-H(4WB)···O(6)	2.844	1.907	171.6	2-x, 1-y, -z

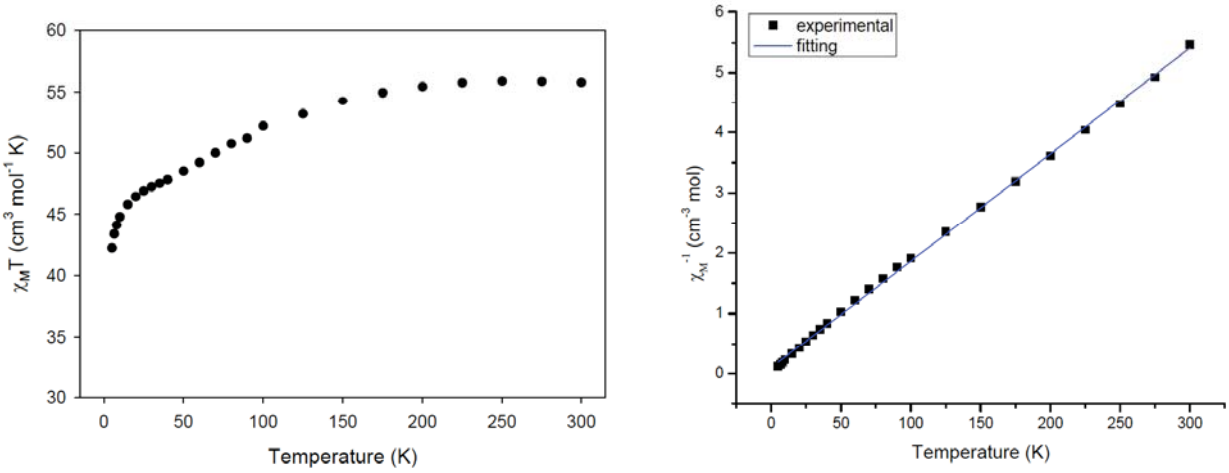

Fig. (5). Plots of $\chi_M T$ vs. T (left) and χ_M^{-1} vs. T (right) for **1**·2PhCO$_2$H·2H$_2$O; the blue thick line represents the fitting of the data to the Curie-Weiss law.

There are few 1-D lanthanide(III) coordination polymers bearing solely monocarboxylate bridging ligands albeit all of them possess a single-chain structural conformation [29, 32]. Complex **1** is the first one-dimensional homometallic Ln(III) coordination polymer with a double-chain architecture consisting of {Ln$^{III}_4$} repeating units. It is difficult to rationalize the chemical reason(s) contributing to such structural difference; however, our ongoing synthetic endeavors reveal that the effect of the reaction solvent(s) on the product's identity is more than pronounced. In particular, the use of exclusively protic solvent media (i.e., ROH; R = various) foster the formation of common 1-D single-chains with [Ln$_2$(O$_2$CPh)$_4$(ROH)$_6$] repeating units [30].

3.3. Magnetochemistry

3.3.1. Direct Current Magnetic Susceptibility Studies

Variable-temperature magnetic susceptibility measurements were performed on a powdered polycrystalline sample of complex **1**·2PhCO$_2$H·2H$_2$O, restrained in eicosane to prevent torquing, in a 1 kG (0.1 T) field and in the 5.0-300 K range. The data are shown as $\chi_M T$ vs. T plot in Fig. (**5**) (left). At 300 K, the $\chi_M T$ value for **1**·2PhCO$_2$H·2H$_2$O is 55.79 cm^{3}Kmol^{-1}, slightly lower than the expected value of 56.68 cm^{3}Kmol^{-1} for four Dy^{III} (S = 5/2, L = 5, g_J = 4/3, ^{6}H$_{15/2}$) non-interacting ions. Upon lowering the temperature, the $\chi_M T$ value of **1**·2PhCO$_2$H·2H$_2$O gradually decreases to a minimum value of 42.22 cm^{3}Kmol^{-1} at 5.0 K. Given (i) the large spin-orbit coupling of Dy^{III} ions, (ii) the fact that the field dependence of the magnetization below 10 K is not saturated even at 7 T, indicative of a significant magnetic anisotropy and/or population of low-lying excited states [31], and (iii) the complicated 1-D double-chain structure of **1**·2*n*(PhCO$_2$H)·*n*(MeCN), it is difficult to conclude the exact strength and nature of the magnetic exchange interactions between the metal centers. Instead, a fit of the experimental data to the Curie-Weiss law at 5-300 K gives a Curie constant, C, of 56.82 cm^{3}Kmol^{-1} and a Weiss temperature, θ, of -5.87 K (Fig. **5**, right). The negative θ value indicates the presence of antiferromagnetic interactions between the Dy^{III} centres [32], very likely mediated through the two *syn,syn*-bridging PhCO$_2^-$ groups (within the individual chains **A** and **B**) and the *syn,anti*-bridging benzoate (between chains **A** and **B**) with separations of 4.925(3)/5.087(3) Å and 5.846(3) Å, respectively. However, as has previously been reported in many examples of Dy^{III}-containing clusters and coordination polymers [9, 19, 20, 31, 32], the orbital contribution induced by the thermal depopulation of the Stark sublevels of the

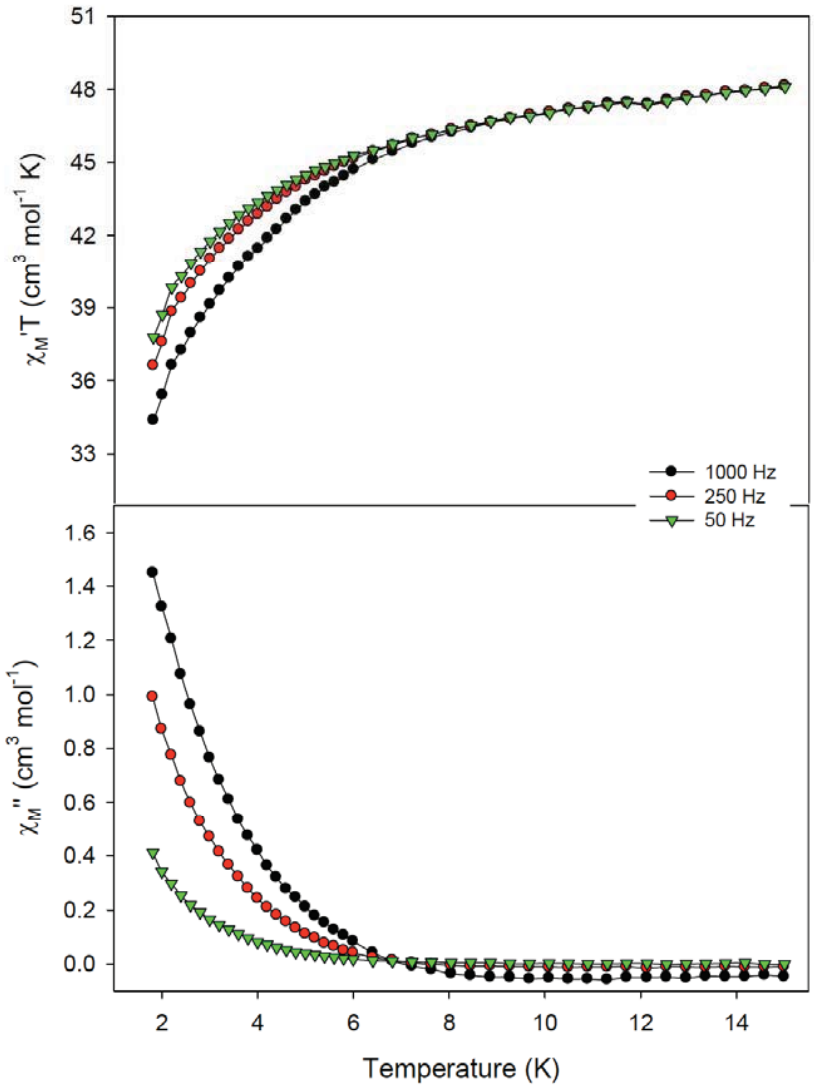

Fig. (6). The in-phase (χ'_M) (as $\chi'_M T$, top) and out-of-phase (χ''_M, bottom) vs. T ac susceptibility signals for **1**·2PhCO$_2$H·2H$_2$O in a 3.5 G field oscillating at the indicated frequencies.

Dy^{3+} ion can also be responsible for the decrease of the $\chi_M T$ product.

In the light of these first observations, alternating current (ac) magnetic susceptibility studies were performed in order to investigate the magnetization dynamics of the 1-D double-chain **1** under a zero dc magnetic field.

3.3.2. Alternating Current Magnetic Susceptibility Studies

Ac studies were performed in the 1.8-15 K range using a 3.5 G ac field oscillating at frequencies in the 50-1000 Hz range. If the magnetization vector can relax fast enough to keep up with the oscillating field, then there is no imaginary (out-of-phase) susceptibility signal (χ''_M), and the real (in-phase) susceptibility (χ'_M) is equal to the dc susceptibility. However, if the barrier to magnetization relaxation is significant compared to thermal energy (kT), then there is a non-zero χ''_M signal and the in-phase signal decreases. In addition, the χ''_M signal will be frequency-dependent. Such frequency-dependent χ''_M signals are a characteristic signature of the superparamagnetic-like properties of a SMM or a SCM (but by themselves do not prove the presence of a SMM/SCM [33]). For complex **1**·2PhCO$_2$H·2H$_2$O, the in-phase $\chi'_M T$ signal (Fig. **6**, top) steadily decreases from 15 K down to approximately 6 K indicating depopulation of a high density of excited states with spin S greater than that of the ground state. Below ~6 K, the decrease in the $\chi'_M T$ vs. T plot is frequency dependent, and there is a concomitant appearance of a frequency-dependent out-of-phase χ''_M signal (Fig. **6**, bottom), whose peak is below the operating minimum of our SQUID magnetometer. Such signals suggest but do not prove that complex **1**·2PhCO$_2$H·2H$_2$O is a SMM/SCM. To confirm this, magnetization vs. dc field sweeps were necessary at temperatures below 1.8 K to look for magnetization hysteresis, the diagnostic property of a magnet.

3.3.3. Magnetization Versus dc Field Hysteresis Loops

Studies were performed on single crystals of **1**·2n(PhCO$_2$H)·n(MeCN) at temperatures down to 0.03 K using a micro-SQUID apparatus. The obtained magnetization vs. applied dc field responses are shown in Fig. (**7**),

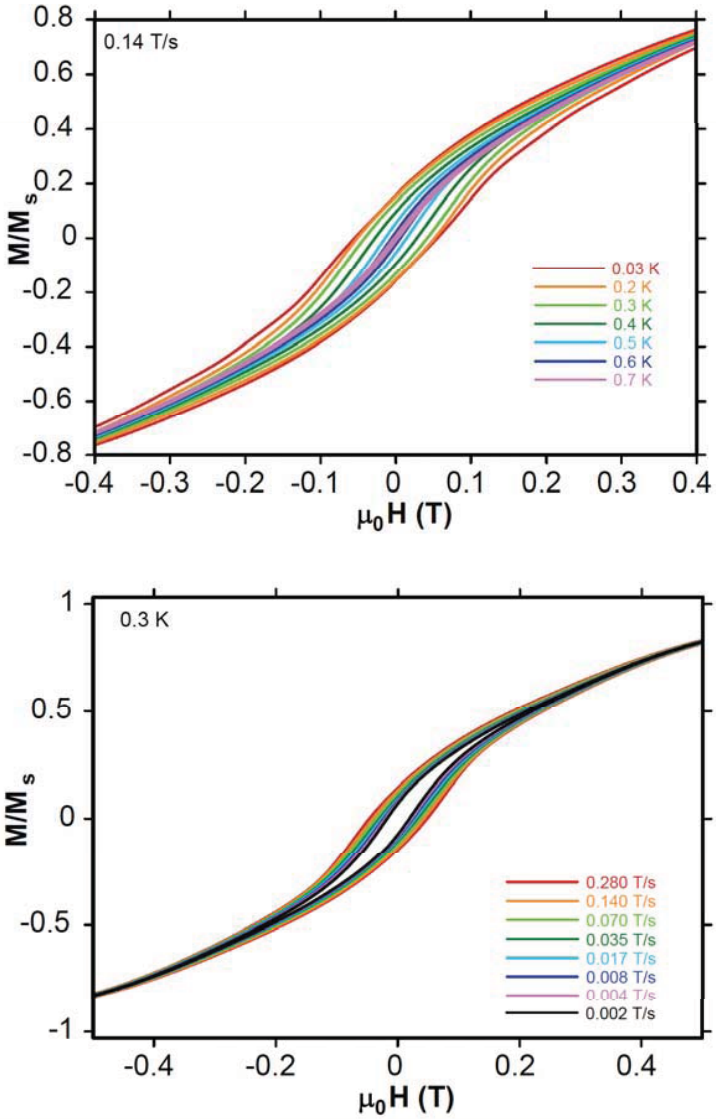

Fig. (7). Magnetization (*M*) vs. dc field hysteresis loops for a single crystal of **1**·2*n*($PhCO_2H$)·*n*(MeCN) at the indicated temperatures and a fixed field sweep rate of 0.14 T/s (top), and at the indicated field sweep rates and a fixed temperature of 0.3 K (bottom). The magnetization is normalized to its saturation value, M_S.

which includes both a temperature dependence at a constant field sweep rate of 0.14 T/s (Fig. **7**, top) and a field sweep rate dependence at a constant temperature of 0.3 K (Fig. **7**, bottom). Hysteresis loops were indeed observed below 0.7 K, whose coercivities increase with decreasing temperature and increasing field sweep rate, as expected for the superparamagnetic-like properties of a SMM (or a SCM [6]) below its blocking temperature (T_B). The data thus confirm complex **1**·2*n*($PhCO_2H$)·*n*(MeCN) to be a new addition to the family of molecular nanomagnets. The blocking temperature (T_B) is ~0.7 K, above which there is no hysteresis. The loops do not show any steps characteristic of quantum tunneling of magnetization (QTM); this is as expected for weakly coupled SMMs and/or SCMs since they are more susceptible to various step-broadening effects from low lying excited states, intermolecular interactions, and/or distributions of local environments owing to ligand and solvent disorder in the often large voids that contain molecules of crystallization [34], as is the case for **1**·2*n*($PhCO_2H$)·*n*(MeCN). The latter distribution of environments leads to a corresponding distribution in *D* values, and thus a broadening of the steps, sometimes to the point of being smeared beyond detection, because their exact position depends on *D*.

Given the complexity of the supramolecular structure of **1**·2*n*($PhCO_2H$)·*n*(MeCN), it is not possible at the current level of our studies to rationalize the exact origin of magnetization relaxation. Undergoing synthetic efforts are oriented toward the isolation of the single-chain version of **1**, that is the 1D chain **A** without the *syn,anti*-bridging benzoate ligands providing magnetic communication between the chains.

4. CONCLUSION AND PERSPECTIVES

In conclusion, we have herein reported the synthesis, structure and complete magnetochemical characterization of

a new one-dimensional coordination polymer possessing a double-chain structure built by $\{Dy^{III}_4\}$ repeating units. The bridging ligation within the double-chain is solely provided by benzoate groups while the terminal ligation is completed by bidentate chelating $PhCO_2^-$ and monodentate H_2O groups, giving rise to different coordination geometries (square antiprismatic vs. triangular dodecahedral) for each crystallographically unique Dy^{III} atom. The lattice structure of **1** is further extended to an interesting 2-D network through hydrogen bonding and π-π stacking interactions. The magnetization hysteresis loops for the described $[Dy_4(O_2CPh)_{12}(H_2O)_8]_n{\cdot}2n(PhCO_2H){\cdot}n(MeCN)$ coordination polymer unequivocally confirm that it is a new molecular nanomagnet.

Finally, the present work serves to emphasize the attention that synthetic inorganic chemists should pay during the preparation of "simple" 3d- and 4f-metal carboxylate precursors that are not commercially available by assuming that the resulting solid compounds would either hold the monomeric $[M(O_2CR)_n]$ (n = 2 for transition metals or 3 for lanthanides; R = various) formulae or exhibit the known $[M_2(O_2CR)_x(H_2O)_y]$ (x = 4, y = 2 for divalent 3d-metals or x = 6, y = 4 for 4f-metals) "paddlewheel" structures. The simple carboxylate character, the absence of any additional bridging groups other than the benzoate ones, the high-yield synthesis, and the good solubility properties make the reported compound a useful starting material in the area of dysprosium carboxylate chemistry with implications in the field of molecular magnetism. It will be interesting to see in the future to what extent this chemistry will include other 4f-metal ions without altering the double-chain structure and the importance of the resulting magnetic properties.

CONFLICT OF INTEREST

The authors confirm that this article content has no conflicts of interest.

ACKNOWLEDGEMENTS

This work was supported by the Ontario Trillium Scholarship (to DIA, ThCS), NSERC (Discovery grant to ThCS), the ERC Advanced Grant MolNanoSpin No. 226558 (to WW), and the National Science Foundation (Grant DMR-1213030 to GC).

SUPPLEMENTARY INFORMATION

CCDC 931712 contains the supplementary crystallographic data for $\mathbf{1}{\cdot}2n(PhCO_2H){\cdot}n(MeCN)$. These data can be obtained free of charge via http://www.ccdc.cam.ac.uk/-conts/retrieving.html or from the Cambridge Crystallographic Data Centre, 12 Union Road, Cambridge CB2 1 EZ, UK; fax: (+44) 1223-336-033; or e-mail: deposit@ccdc.cam.ac.uk.

REFERENCES

[1] Constable, E. C.; Housecroft, C. E. Coordination chemistry: the scientific legacy of Alfred Werner. *Chem. Soc. Rev.,* **2013**, *42*, 1429-1439.

[2] (a) Sessoli, R.; Powell, A. K. Strategies towards single molecule magnets based on lanthanide ions. *Coord. Chem. Rev.*, **2009**, *253*, 2328-2341. (b) Luzon, J.; Sessoli, R. Lanthanides in molecular magnetism: so fascinating, so challenging. *Dalton Trans.,* **2012**, *41*, 13556-13567. (c) Bünzli, J.C.G.; Eliseeva, S.V. Intriguing aspects of lanthanide luminescence. *Chem. Sci.,* **2013**, article in press.

[3] Janiak, C. Engineering coordination polymers towards applications. *Dalton Trans.*, **2003**, 2781-2804.

[4] Gómez-Romero, P.; Sanchez, C. *Functional Hybrid Materials*; Wiley-VCH: Weinheim, Germany, **2004**.

[5] Christou, G.; Gatteschi, D.; Hendrickson, D. N.; Sessoli, R. Single-molecule magnets. *MRS Bull.*, **2000**, *25*, 66-71.

[6] (a) Miyasaka, H.; Clérac, R. Synthetic strategy for rational design of single-chain magnets. *Bull. Chem. Soc. Jpn.*, **2005**, *78*, 1727-1748. (b) Coulon, C.; Miyasaka, H.; Clérac, R. Single-chain magnets: Theoretical approach and experimental systems. *Struct. Bonding (Berlin),* **2006**, *122*, 163-206.

[7] Coronado, E.; Day, P. Magnetic molecular conductors. *Chem. Rev.,* **2004**, *104*, 5419-5448. (b) Bogani, L.; Wernsdorfer, W. Molecular spintronics using single-molecule magnets. *Nature Mat.,* **2008**, *7*, 179-186.

[8] Aromí, G.; Aguilà, D.; Gamez, P.; Luis, F.; Roubeau, O. Design of magnetic coordination complexes for quantum computing. *Chem. Soc. Rev.*, **2012**, *41*, 537-546.

[9] Habib, F.; Murugesu, M. Lessons learned from dinuclear lanthanide nano-magnets. *Chem. Soc. Rev.*, **2013**, *42*, 3278-3288.

[10] Winpenny, R.E.P. Comprehensive Coordination Chemistry II, Vol. 7, (Eds.: J. A. McCleverty, T. J. Meyer), Elsevier, Amsterdam, **2004**, pp. 125-175.

[11] Papaefstathiou, G. S.; Perlepes, S. P. Families of polynuclear manganese, cobalt, nickel and copper complexes stabilized by various forms of di-2-pyridyl ketone. *Comments Inorg. Chem.,* **2002**, *23*, 249-274.

[12] Stamatatos, Th. C.; Efthymiou, C. G.; Stoumpos, C. C.; Perlepes, S. P. Adventures in the coordination chemistry of di-2-pyridyl ketone and related ligands: From high-spin molecules and single-molecule magnets to coordination polymers, and from structural aesthetics to an exciting new reactivity chemistry of coordinated ligands. *Eur. J. Inorg. Chem.*, **2009**, 3361-3391.

[13] Wernsdorfer, W. Classical and quantum magnetization reversal studied in nanometer-sized particles and clusters *Adv. Chem. Phys.,* **2001**, *118*, 99-190.

[14] *Crystal Clear*, Rigaku/MSC Inc, The Woodlands, Texas, USA, **2005**.

[15] Sheldrick, G. M. SHELXS-97, *Structure Solving Program*, University of Göttingén, Germany, **1997**.

[16] Sheldrick, G. M. SHELXL-97, *Program for the Refinement of Crystal Structures from Diffraction Data*, University of Göttingén, Germany, **1997**.

[17] *Mercury;* Bruno, I. J.; Cole, J. C.; Edgington, P. R.; Kessler, M. K.; Macrae, C. F.; McCabe, P.; Pearson, J.; Taylor, R. *Acta Crystallogr., Sect. B,* **2002**, *58*, 389.

[18] Bradenburg, K. *DIAMOND, Release 3.1f, Crystal Impact GbR*; Bonn, Germany, **2008**.

[19] Alexandropoulos, D.I.; Mukherjee, S.; Papatriantafyllopoulou, C.; Raptopoulou, C.P.; Psycharis, V.; Bekiari, V.; Christou, G.; Stamatatos, Th. C. A new family of nonanuclear lanthanide clusters displaying magnetic and optical properties. *Inorg. Chem.*, **2011**, *50*, 11276-11278.

[20] For some representative references, see: (a) Canaj, A.B.; Tzimopoulos, D.I.; Philippidis, A.; Kostakis, G.E.; Milios, C.J. A strongly blue-emitting heptametallic $[Dy^{III}_7]$ centered-octahedral single-molecule magnet. *Inorg. Chem.*, **2012**, *51*, 7451-7453. (b) Chilton, N.F.; Langley, S.K.; Moubaraki, B.; Soncini, A.; Batten, S.R.; Murray, K.S. Single molecule magnetism in a family of mononuclear β-diketonate lanthanide(III) complexes: rationalization of magnetic anisotropy in complexes of low symmetry. *Chem. Sci.,* **2013**, *4*, 1719-1730. (c) Hewitt, I.J.; Tang, J.; Madhu, N.T.; Anson, C.E.; Lan, Y.; Luzon, J.; Etienne, M.; Sessoli, R.; Powell, A.K. Coupling Dy_3 triangles enhances their slow magnetic relaxation. *Angew. Chem. Int. Ed.,* **2010**, *49*, 6352-6356.

[21] Zoan, T.A.; Kuzmina, N.P.; Frolovskaya, S.N.; Rykov, A.N.; Mitrofanova, N.D.; Troyanov, S.I.; Pisarevsky, A.P.; Martynenko, L.I.; Korenev, Y.M. Synthesis, structure and properties of volatile lanthanide pivalates. *J. Alloys Compd.*, **1995**, *225*, 396-399.

[22] Nakamoto, K. Infrared and Raman spectra of inorganic and coordination compounds. 4th ed., Wiley, New York, **1986**, pp. 229, 254-257.

[23] Stamatatos, Th. C.; Katsoulakou, E.; Nastopoulos, V.; Raptopoulou, C.P.; Manessi-Zoupa, E.; Perlepes, S.P. Cadmium carboxylate

chemistry: Preparation, crystal structure, and thermal and spectroscopic characterization of the one-dimensional polymer $[Cd(O_2CMe)(O_2CPh)(H_2O)_2]_n$. *Z. Naturforsch*. **2003**, *58b*, 1045-1054.

[24] (a) Milios, C.J.; Stamatatos, Th. C.; Kyritsis, P.; Terzis, A.; Raptopoulou, C.P.; Vicente, R.; Escuer, A.; Perlepes, S.P. Phenyl 2-pyridyl ketone and its oxime in manganese carboxylate chemistry: synthesis, characterization, x-ray studies and magnetic properties of mononuclear, trinuclear and octanuclear complexes. *Eur. J. Inorg. Chem.*, **2004**, 2885-2901. (b) Deacon, G.B.; Phillips, R.J. Relationships between the carbon-oxygen stretching frequencies of carboxylato complexes and the type of carboxylate coordination. *Coord. Chem. Rev.*, **1980**, *33*, 227-250.

[25] Llunell, M.; Casanova, D.; Girera, J.; Alemany, P.; Alvarez, S. *SHAPE*, version 2.0, Barcelona, Spain, **2010**.

[26] Zabrodsky, H.; Peleg, S.; Avnir, D. Continuous symmetry measures. *J. Am. Chem. Soc.*, **1992**, *114*, 7843-7851.

[27] Ruiz-Martinez, A.; Casanova, D.; Alvarez, S. Polyhedral structures with an odd number of vertices: Nine-coordinate metal compounds. *Chem. Eur. J.*, **2008**, *14*, 1291-1303.

[28] Zabrodsky, H.; Peleg, S.; Avnir, D. Continuous symmetry measures. 2. Symmetry groups and the tetrahedron. *J. Am. Chem. Soc.*, **1993**, *115*, 8278-8289.

[29] (a) Song, Y.S.; Yan, B.; Weng, L.H. Four distinctive 1-D lanthanide carboxylate coordination polymers: Synthesis, crystal structures and spectral properties. *Polyhedron*, **2007**, *26*, 4591-4601. (b) Luo, Y.; Sun, G.; Li, D.; Luo, F. 1D ferromagnetic Dy(III) compound showing supramolecular four-connecting rod-packing architecture. *Inorg. Chem. Commun.*, **2011**, *14*, 778-780.

[30] Alexandropoulos, D.I.; Stamatatos, Th. C. Unpublished results.

[31] Lin, P.H.; Burchell, T.J.; Ungur, L.; Chibotaru, L.F.; Wernsdorfer, W.; Murugesu, M. A polynuclear lanthanide single-molecule magnet with a record anisotropic barrier. *Angew. Chem. Int. Ed.*, **2009**, *48*, 9489 -9492.

[32] (a) Luo, F.; Liao, Z.; Song, Y.; Huang, H.; Tian, X.; Sun, G.; Zhu, Y.; Yuan, Z.Z.; Luo, M.; Liu, S.; Xu, W.; Feng, X.F. Chiral 1D Dy(III) compound showing slow magnetic relaxation. *Dalton Trans.*, **2011**, *40*, 12651-12655. (b) Majeed, Z.; Mondal, K.C.; Kostakis, G.E.; Lan, Y.; Anson, C.E.; Powell, A.K. $[LnNa(PhCO_2)_4]$ (Ln = Ho, Dy): the first examples of chiral srs 3D networks constructed using the monotopic benzoate ligand. *Chem. Commun.*, **2010**, *46*, 2551-2553.

[33] Chakov, N.E.; Wernsdorfer, W.; Abboud, K.A.; Christou, G. Mixed-valence $Mn^{III}Mn^{IV}$ clusters $[Mn_7O_8(O_2SePh)_8(O_2CMe)(H_2O)]$ and $[Mn_7O_8(O_2SePh)_9(H_2O)]$: Single-chain magnets exhibiting quantum tunneling of magnetization. *Inorg. Chem.*, **2004**, *43*, 5919-5930. (b) Mishra, A.; Tasiopoulos, A.J.; Wernsdorfer, W.; Abboud, K. A.; Christou, G. High-nuclearity Ce/Mn and Th/Mn cluster chemistry: Preparation of complexes with $[Ce_4Mn_{10}O_{10}(OMe)_6]^{18+}$ and $[Th_6Mn_{10}O_{22}(OH)_2]^{18+}$ cores. *Inorg. Chem.*, **2007**, *46*, 3105-3115.

[34] Moushi, E.E.; Lampropoulos, C.; Wernsdorfer, W.; Nastopoulos, V.; Christou, G.; Tasiopoulos, A. J. Inducing single-molecule magnetism in a family of loop-of-loops aggregates: Heterometallic $Mn_{40}Na_4$ clusters and the homometallic Mn_{44} analogue. *J. Am. Chem. Soc.*, **2010**, *132*, 16146-16155.

Received: April 02, 2013 Revised: April 18, 2013 Accepted: April 19, 2013